

Dynamic Aware: Adaptive Multi-Mode Out-of-Distribution Detection for Trajectory Prediction in Autonomous Vehicles

Tongfei Guo¹ and Lili Su¹

Abstract—Trajectory prediction is central to the safe and seamless operation of autonomous vehicles (AVs). In deployment, however, prediction models inevitably face distribution shifts between training data and real-world conditions, where rare or underrepresented traffic scenarios induce out-of-distribution (OOD) cases. While most prior OOD detection research in AVs has concentrated on computer vision tasks such as object detection and segmentation, trajectory-level OOD detection remains largely underexplored. A recent study formulated this problem as a quickest change detection (QCD) task, providing formal guarantees on the trade-off between detection delay and false alarms [1]. Building on this foundation, we propose a new framework that introduces adaptive mechanisms to achieve robust detection in complex driving environments. Empirical analysis across multiple real-world datasets reveals that prediction errors—even on in-distribution samples—exhibit mode-dependent distributions that evolve over time with dataset-specific dynamics. By explicitly modeling these error modes, our method achieves substantial improvements in both detection delay and false alarm rates. Comprehensive experiments on established trajectory prediction benchmarks show that our framework significantly outperforms prior UQ- and vision-based OOD approaches in both accuracy and computational efficiency, offering a practical path toward reliable, driving-aware autonomy.

I. INTRODUCTION

Trajectory prediction is a cornerstone of autonomous vehicle’s (AV’s) seamless operation, as errors in forecasting the movements of surrounding agents may cascade through the downstream autonomy stack, ultimately leading to incorrect maneuvers. Despite advances in deep learning, their real-world deployments inevitably encounter a mismatch between the training data and the deployment environment. This mismatch (a.k.a., distribution shift) may stem from various practical factors. For example, due to the data collection and annotation complexity, large-scale datasets tend to overrepresent routine scenarios – such as highway driving or straight-lane trajectories – while underrepresenting complex and diverse environments, including multi-lane intersections and roundabouts [2], [3]. Moreover, real-world driving inherently harbors a wide range of uncertainties, such as sudden braking, falling obstacles, or adversarial behaviors by other drivers. These rare or unseen conditions give rise to out-of-distribution (OOD) traffic scenes, where prediction models are prone to generating overconfident yet erroneous forecasts that jeopardize safety.

*This work was not supported by any organization

¹Department of Electrical and Computer Engineering, Northeastern University, Boston, MA, USA. {guo.t, l.su}@northeastern.edu

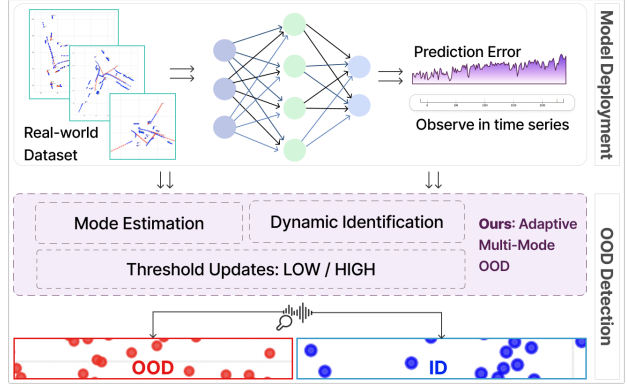


Fig. 1: Illustration of our adaptive multi-mode OOD detection framework for trajectory prediction in AVs.

Existing research on OOD detection in AVs has primarily focused on traditional computer vision tasks such as object detection and semantic segmentation [4], [5], with representative approaches including post-hoc scoring [6], feature-space density estimation [7], and energy-based models [8]. These methods are predominantly frame-wise. A key limitation of this frame-wise approach is that it determines whether the ego vehicle is in an in-distribution (ID) or OOD traffic scene solely based on information from the current frame, thereby overlooking the spatiotemporal correlations among the trajectories of surrounding agents. As a consequence, frame-wise approaches tend to perform well only when the distance between ID and OOD data is sufficiently large, resulting in significantly suboptimal detection performance in the more challenging yet practical setting where the deviations between OOD and ID scenes are minor at individual frames but may gradually escalate into hazardous situations if left unnoticed. Such cases are referred to as **deceptive OOD scenarios** [1], which are the focus of this paper.

While uncertainty quantification (UQ) could help guide OOD detection [4], [5], [9], existing methods mostly lack theoretical guarantees. Observing the sequential nature of traffic scenes, a recent work formulated the trajectory OOD detection as a quickest change detection problem [1]. They extended the *light-weight* cumulative sum (CUSUM) method to detect deceptive OOD for trajectory prediction, which can provide formal guarantees on the trade-off between detection delay and false alarms under comparable or more relaxed probabilistic assumptions than UQ. In this work, we build on [1] and advance the framework by introducing new mechanisms to achieve adaptive and robust detection in

complex driving environments.

Contributions. Our main contributions are:

- We first observe, across multiple popular real-world datasets, that prediction errors – even on ID samples – exhibit *mode-dependent* (high/low error modes) distributions, and that the error modes evolve over time, potentially following different dynamics across datasets.
- We extend the QCD-based formulation to incorporate mode dynamics.
- We propose a *Mode-Aware* OOD detection method that adapts to diverse driving contexts by employing scene-specific detection declaration thresholds. Our design is modular and is compatible with a broad range of models and distributions.
- We validate our approach through extensive experiments on established trajectory prediction benchmarks. Results demonstrate that our *Mode-Aware* detection method improves both detection delay and false alarm rates compared with the non-adaptive method, consistently outperforming existing UQ- and vision-based OOD methods at a lower computation cost.

II. RELATED WORK

Trajectory Prediction. Trajectory prediction is a critical component in autonomous driving. Early approaches relied on recurrent neural networks (RNNs) [10], [11], to model single-agent behavior, while subsequent work introduced interaction-aware mechanisms such as social pooling and graph-based models to capture multi-agent dependencies [12], [13]. More recently, advanced methods have increasingly adopted Transformer architectures [14], [15], [16] and spatio-temporal graph neural networks [17] to improve accuracy, enable real-time forecasting, and capture complex interactions. Despite these advances, the reliability of trajectory prediction under distribution shifts remains relatively underexplored. A small number of studies address related issues through uncertainty estimation [18], [19] and adversarial attacks [20], [21]. Robustness to OOD samples is increasingly recognized as a fundamental performance indicator for trajectory prediction models [22]. However, comprehensive approaches for OOD detection in trajectory prediction remain relatively underexplored.

OOD Detection in AVs. Most existing OOD detection research in AVs has primarily focused on perception tasks such as object detection, semantic segmentation, and depth estimation [4], [5], [9]. Representative approaches include scoring functions such as maximum softmax probability (MSP) [23] and energy-based scores [8], as well as latent-space density estimation techniques [24], [25]. These OOD detection methods are not fully suited for trajectory prediction since they overlook the spatiotemporal correlations among the trajectories of surrounding agents. Moreover, as summarized in [26], prevailing OOD performance metrics often prioritize recognition accuracy without addressing detection delay and computation complexity.

Application of UQ to OOD Detection. Popular UQ for trajectory prediction [27], [28], [29] include deep ensembles,

Monte Carlo dropout, and Bayesian neural networks. While effective, these methods typically incur substantial computational overhead. Recent research has focused on developing more efficient UQ frameworks tailored for OOD detection. For instance, [18] introduced a scalable approach that models ID samples within a latent space using a Gaussian Mixture Model (GMM), identifying OOD samples as low-likelihood outliers—a principle shared by other density-based detection methods [24], [25]. Complementarily, [1] introduced an external monitoring module that operates directly on model outputs, detecting OOD samples via prediction error statistics without altering the underlying predictor.

Quickest Change-Point Detection (QCD). QCD provides a rigorous framework for monitoring sequential data to identify the *change-point* at which its underlying distribution shifts, with the dual objectives of minimizing the detection delay and controlling the frequency of false alarms [30]. This formalism, with applications spanning finance, climatology, and network monitoring [31], [32], [33], is typically pursued within either a Bayesian [34] or minimax [35] setting. In particular, CUSUM algorithm is first-order asymptotically optimal [36], [37], [30]. These strong theoretical guarantees, combined with its computational efficiency and proven effectiveness in time-sensitive applications [38], [39], make CUSUM a powerful and principled foundation for our work.

III. MODE-DEPENDENT PREDICTION ERROR DISTRIBUTIONS

We observe, across diverse real-world datasets, prediction errors—even on ID samples—exhibit *mode-dependent* (high/low modes) distributions that evolve over time with dataset-specific dynamics. We conjecture that this mode-dependent behavior of prediction errors is not dataset-specific but may generalize to a broader spectrum of ML models and trajectory prediction datasets. Moreover, the set of modes may extend beyond two, potentially encompassing a more general and richer class of modes.

A. Overall Multiple Error Modes

We begin with an empirical study of prediction errors across multiple trajectory models (e.g., GRIP++ [40], FQA [41]) and datasets (ApolloScape [42], NGSIM [43], nuScenes [44]). These three datasets vary in map topology, traffic composition, and density. Specifically, NGSIM provides long highway trajectories, ApolloScape contains urban driving scenarios with heterogeneous traffic-agents in Beijing metropolitan areas, and nuScenes mainly involves data collected in Boston and Singapore, both cities are known for dense and varied traffic. Further details on these datasets are provided in Section VI-A.

As illustrated in Fig. 2, the overall prediction errors for each of the datasets are well approximated by a GMM that naturally divides into two latent components: a *low-risk mode* component and a *high-risk mode* component. The relative weights of these modes vary substantially across datasets and across models. For GRIP++, the low-/high-risk proportions are 44.1%/55.9% (ApolloScape), 59.9%/40.1%

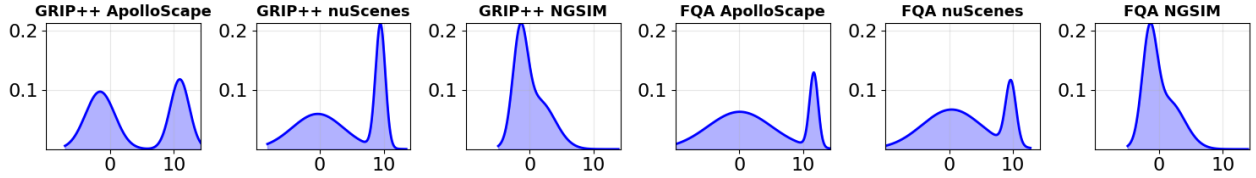


Fig. 2: Observed Gaussian mixture distribution across models and datasets.

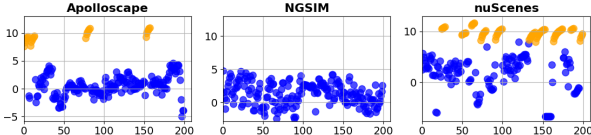


Fig. 3: Mode dynamics across different driving scenes for FQA. Datasets include ApolloScape, NGSIM, and nuScenes. The x-axis is time, the y-axis is error magnitude (log scale). Low-risk (blue) vs high-risk (orange).

(nuScenes), and 48.4%/51.6% (NGSIM). For FQA, they are 79.1%/20.9% (ApolloScape), 78.0%/22.0% (nuScenes), and 43.4%/56.6% (NGSIM). It is worth noting that in Fig. 2, FQA tends to have smaller weights on the high-risk mode on both ApolloScape and nuScenes. We conjecture that this is because FQA’s special fuzzy attention can better capture the complex agent-agent and agent-map interactions in those datasets.

B. On the Temporal Evolution of Error Modes

We observe that the error modes evolve over time, potentially following different dynamics across datasets. Intuitively, in highway driving scenes, the ego vehicle often remains in the same error mode for long, consecutive periods, with only occasional transitions. In contrast, dense urban intersections feature more abrupt and frequent behavioral changes from surrounding agents, resulting in higher switching rates between low- and high-risk modes. Our experimental results align with this intuition, as is shown in Fig. 3:

- **ApolloScape and nuScenes:** Urban intersection settings where close-proximity interactions drive frequent and abrupt mode shifts.
- **NGSIM:** Highway settings where prediction errors predominantly remain in the low-risk mode, with occasional high-risk episodes likely corresponding to low-frequency maneuvers such as lane changes or merging.

The mode dynamics under GRIP++ are expected to be somewhat similar to those in Fig. 3 yet with overall higher frequency in high-risk mode in ApolloScape and nuScenes. Due to space constraints, we leave the corresponding experiments to the full version.

C. Limitations of Vision-Based Error Mode Identification

Due to the inherent randomness of prediction errors, the underlying error mode is not directly observable. Moreover, readily available scene-level statistics – such as agent counts, maximum/average speeds, or map snapshots – offer no reliable cues for identifying mode transitions, as is shown

in Fig. 4. Specifically, the mode transitions (highlighted in dashed pink lines) occur without corresponding changes in the plots: agent density remains stable, speed metrics show no anomalous patterns, and the scene snapshots display consistent visual characteristics. The lack of significant correlations undermines the foundation for using purely vision-based solutions to infer the unknown error mode.

IV. PROBLEM FORMULATION

In this section, we provide a mathematical description of the mode-dependent QCD problem. Observing the near-Gaussian mixture distributions with two modes in Fig. 2, we formulate the problem for the two-mode case. Our formulation can be naturally extended to an arbitrary number of modes.

A. Overall Error Distribution

Let ε denote the prediction error. Let $f(\cdot)$ denote the overall error distribution in the training dataset. For ease of exposition, we assume the training dataset is sufficiently large so that f can be treated as a probability density function (pdf). Let $\mathcal{M} = \{0, 1\}$ denote the two possible modes, with 0 indicating low-error mode, and 1 indicating high-error mode. Suppose that f is a mixture distribution of two components, formally $f(X) = \pi_0 f_0(X) + \pi_1 f_1(X)$, where $\pi_0 \geq 0$, $\pi_1 \geq 0$, and $\pi_0 + \pi_1 = 1$. The supports of f_0 and f_1 may overlap with each other. For example, when f is Gaussian mixture, the supports of f_0 and f_1 are both the entire \mathbb{R} . Without loss of generality, we assume $\mathbb{E}_{\varepsilon \sim f_0}[\varepsilon] < \mathbb{E}_{\varepsilon \sim f_1}[\varepsilon]$. We assume that f is fully specified and known to the ego vehicle.

B. Mode Dynamics

Let $M_t \in \mathcal{M}$ denote the mode of the ego vehicle at timestep t for $t = 0, 1, \dots$, which is unobservable and its evolution over time is unknown. In the real world, there can be a wide range of possible dynamics. Some representative examples are as follows:

- *Static & random initialization:*

$$M_t = M_1 \quad \forall t \geq 1, \text{ and } \mathbb{P}\{M_1 = 0\} = \pi_0 = 1 - \pi_1. \quad (1)$$

The physical meaning of this dynamics is that: after entering a sufficiently long road segment, the error mode remains stable for a sufficiently long time. It may capture the highway scenarios with light traffic.

- *Independent and identically distributed (IID):* For all $t \geq 1$,
- $$\mathbb{P}\{M_t = 0\} = \pi_0 = 1 - \pi_1, \quad \text{and} \quad \mathbb{P}\{M_t = m, \& M_{t'} = m'\} = \mathbb{P}\{M_t = m\} \mathbb{P}\{M_{t'} = m'\}. \quad (2)$$

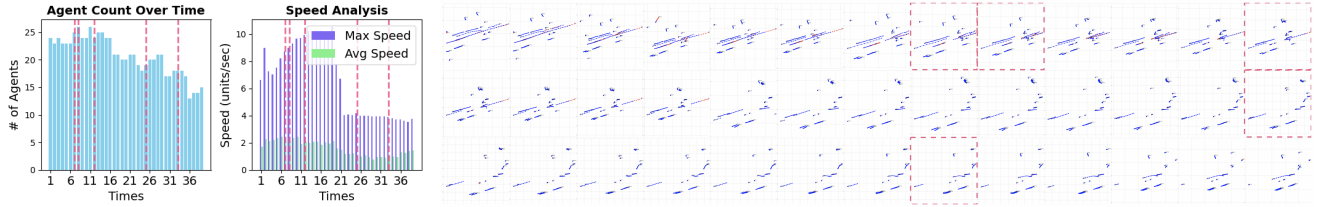


Fig. 4: Scene-level statistics provide limited cues for error modes and their transitions. The figure illustrates (i) agent counts over time, (ii) maximum and average speeds over time, and (iii) corresponding map snapshots of the driving scenes. The pink dashed lines indicate where a mode switch occurs.

That is, mode switches independently at each time, capturing environments with moderate variability, such as suburban arterial roads where interactions occur sporadically.

- *Markovian*: For all $t \geq 1$,

$$\begin{aligned} \mathbb{P}\{M_t \mid M_{t-1}, \dots, M_0\} &= \mathbb{P}\{M_t \mid M_{t-1}\}, \\ \lim_{t \rightarrow \infty} \mathbb{P}\{M_t = 0\} &= \pi_0 = 1 - \pi_1. \end{aligned} \quad (3)$$

That is, the current mode M_t depends on the past only through the most recent mode M_{t-1} . It can be useful to capture structured but non-deterministic driving environments such as urban intersections, where vehicles often linger in one mode before transitioning to another with context-dependent probabilities.

- *Arbitrary given*: Let $t_1, t_2, \dots, t_r, \dots$ denote a given sequence of time indices at each of which there is an error mode switch. Without loss of generality, let $t_1 = \inf\{t : M_t = 1\}$ denote the first time that the M_t enters mode 1. If $t_1 = 1$, then the process starts in mode 1 and switches to mode 0 at time t_2 , and so on. If $t_1 \neq 1$, then the process starts in mode 0 and switches to mode 1 at time t_1 , etc. To align with the overall error distribution f , the given sequence should obey the following condition:

$$\lim_{t \rightarrow \infty} \frac{1}{t} \sum_{r=1}^t \mathbf{1}\{M_r = 0\} = \pi_0, \text{ and } \lim_{t \rightarrow \infty} \frac{1}{t} \sum_{r=1}^t \mathbf{1}\{M_r = 1\} = \pi_1.$$

This dynamic contains the above dynamics as special cases.

C. Change-point Detection

Let γ denote the unknown change-point upon which the ego vehicle starts to enter OOD driving scenarios. Let f_t denote the distribution of ε_t if $t \leq \gamma$. For clarity, we assume a global post-change distribution, denoted by g , and leave the more general setting for future exploration. For simplicity, we assume that ε_t only depends on M_t , and may be dependent on other $\varepsilon_{t'}$ through M_t . In particular, $f_t = f_0$ if $M_t = 0$, $f_t = f_1$ otherwise. Formally,

$$\varepsilon_t \sim \begin{cases} f_t(\cdot), & t < \gamma \\ g(\cdot), & t \geq \gamma. \end{cases}$$

A detection rule τ declares OOD at time τ . For robustness, we adopt Lorden's minimax criterion [37], defining the *Worst-Case Average Detection Delay (WADD)*:

$$\text{WADD}(\tau) = \sup_{t \geq 1} \text{ess} \sup \mathbb{E}_t \left[(\tau - t + 1)^+ \mid \varepsilon_1, \dots, \varepsilon_{t-1} \right],$$

where $(x)^+ = \max\{0, x\}$ and $\mathbb{E}_t[\cdot]$ denotes expectation when the change occurs at t .

False alarms are quantified by the *False Alarm Rate (FAR)* and its reciprocal, the *Mean Time to False Alarm (MTFA)*:

$$\text{FAR}(\tau) = \frac{1}{\mathbb{E}_\infty[\tau]}, \quad \text{MTFA}(\tau) = \mathbb{E}_\infty[\tau],$$

where \mathbb{E}_∞ denotes expectation under the null hypothesis (no change occurs).

The objective is to design a τ that minimizes $\text{WADD}(\tau)$ subject to $\text{FAR}(\tau) \leq \Delta$, for some tolerance $\Delta > 0$.

D. Specification of prediction errors

In trajectory prediction, ε_t can possibly be defined in multiple ways, depending on the metrics chosen to evaluate the trajectory prediction models. We adopt three standard metrics [45], [46]:

- *Average Displacement Error (ADE)*: mean ℓ_2 distance between predicted and ground-truth positions across the prediction horizon.
- *Final Displacement Error (FDE)*: ℓ_2 distance at the final prediction step, highlighting long-horizon accuracy.
- *Root Mean Squared Error (RMSE)*: square root of the average squared deviation, which penalizes large errors and is sensitive to outliers or abrupt shifts.

V. METHOD: ADAPTIVE MULTI-THRESHOLD CHANGE-POINT DETECTION

Building on the experimental findings and formulation in Sections IV-B and IV, we propose an *adaptive multi-threshold change-point detection algorithm (Mode-Aware CUSUM)*, formally described in Algorithm 1. Unlike the mode-agnostic approach in [1], which detects deceptive OOD instances using the overall error distribution as the pre-change distribution, our method explicitly adapts to the underlying latent error mode. Notably, there are some studies on QCD with state-dependent pre-change distributions in the sequential analysis literature [47]. However, existing methods are not directly applicable to our setting. They are either computationally heavy (e.g., the GLR scheme) or rely on exact knowledge of the underlying dynamics, which is unavailable in our problem.

Algorithm 1: Mode-Aware CUSUM

Input: Overall error distribution on the training data f (with π_0, π_1, f_0, f_1); post-change distribution g ; tuning parameters (b_0, b_1) , (r_0, r_1) , $\{(\alpha_m, \beta_m)\}_{m \in \{0,1\}}$, S , and λ

Output: Change point τ if detected

Initialize $W_0^{(0)} \leftarrow 0$, $W_0^{(1)} \leftarrow 0$;

Initialize thresholds $\theta_0^{(0)} \leftarrow b_0$, $\theta_1^{(0)} \leftarrow b_1$;

while true **do**

```

    /* Step 1: mode estimation
     $\hat{M}_t \leftarrow \mathcal{T}(\varepsilon_1, \dots, \varepsilon_t, \pi_0, \pi_1)$  ;
    /* Step 2: compute log-likelihood ratio
     $\ell_t = \ln \frac{g(\varepsilon_t)}{f_{\hat{M}_t}(\varepsilon_t)}$  ;
    /* Step 3: update thresholds (adaptive step-down
    policy) */
    Estimate  $\varepsilon_t$  variance  $\hat{\sigma}^{(\hat{M}_t)}$  over sliding window  $S$ ;
     $d_{\hat{M}_t} \leftarrow r_{\hat{M}_t} \hat{\sigma}^{(\hat{M}_t)}$  ;
     $k_{\hat{M}_t} \leftarrow d_{\hat{M}_t} / 2$  ;
     $h_{\hat{M}_t} \leftarrow \frac{2}{d_{\hat{M}_t}^2} \ln \left( \frac{1 - \beta_{\hat{M}_t}}{\alpha_{\hat{M}_t}} \right)$  ;
     $\theta_t^{(\hat{M}_t)} \leftarrow \lambda h_{\hat{M}_t} + (1 - \lambda) \theta_{t-1}^{(\hat{M}_t)}$  ;
    /* Step 4: update CUSUM statistic for active
    mode */
     $W_t^{(\hat{M}_t)} \leftarrow \max(W_{t-1}^{(\hat{M}_t)} + (\ell_t - k_{\hat{M}_t}), 0)$  ;
    /* Step 5: detection */
    if  $W_t^{(\hat{M}_t)} \geq \theta_t^{(\hat{M}_t)}$  then
        Declare a change point;
        return  $\tau = t$ ;
```

Inputs. Our algorithm inputs contain (1) the full specification of the overall error distribution f , (2) the post-change distribution g , and (3) a collection of tuning parameters.

Inputs (1) and (2) are typical in the QCD literature [30], [31], [32], [33], [36], [37]. In practice, obtaining such prior knowledge depends on the application domain. In our autonomous driving scenario, the overall pre-change distributions can be derived from the training dataset; as we did in Section III-A. Post-change knowledge, when available, is informed by domain expertise, analysis of incident logs, and simulation of adversarial or atypical driving situations. We acknowledge that, in many real-world settings, full information on g may not be available, and we plan to explore this more general setting in future work. Our results demonstrate the potential significance of incorporating error mode dynamics to enhance the performance of deceptive OOD detection.

We will discuss the choices of the tuning parameters together with our major algorithmic components.

Algorithmic Components. Algorithm 1 comprises three interwoven components:

- 1) *Mode estimation.* Let \hat{M}_t denote the estimate at timestep t . We encapsulate the mode estimation component by a generic function \mathcal{T} , which takes all the observed errors

so far $\varepsilon_1, \dots, \varepsilon_t$, and the mode prior (π_0, π_1) as inputs. Its default form is the maximum a posteriori (MAP) estimation method of the current prediction error ε_t , which is optimal when the mode dynamic is arbitrary and no side information is available [48]. If the dynamic has a benign structure Hidden Markov Model (HMM), and sufficient side information is available, one can use off-the-shelf algorithms such as the Viterbi algorithm and its variants.

- 2) *Thresholds update.* The initial thresholds $\theta_0^{(0)} = b_0$ and $\theta_1^{(0)} = b_1$ need to be set properly to control false alarms for the first few timesteps. For each t , we use the adaptive step-down policy. Intuitively, there are two base thresholds $\ln \frac{1 - \beta_0}{\alpha_0}$ and $\ln \frac{1 - \beta_1}{\alpha_1}$ – one for each mode. Specifically, these logarithmic thresholds originate from the sequential probability ratio test (SPRT) in the Neyman-Pearson framework for hypothesis testing, where they define the boundaries for deciding between two hypotheses while controlling the false alarm rate (α) and the missed detection rate (β) [37], [30]. The ego vehicle tends to lean towards the threshold that is proportional to $\ln \frac{1 - \beta_{\hat{M}_t}}{\alpha_{\hat{M}_t}}$. Yet, due to the randomness in ε_t , two tricks are introduced to ensure stability: (a) use exponential smoothing λ to control the innovation added in each timestep, and (b) adaptively scale the base threshold based on the estimation error variance – the larger the variance, the smaller the essential weight of $\ln \frac{1 - \beta_{\hat{M}_t}}{\alpha_{\hat{M}_t}}$. The heterogeneous constant tuning parameters r_0 and r_1 allow us to ensure different sensitivities to the error modes. In particular, we choose $r_0 > r_1$ to implement a conservative threshold in the low-error mode to absorb frequent mode switches.
- 3) *Adaptive multi-mode detection with dynamic awareness.* The corresponding CUSUM statistic is first updated using a one-step CUSUM update that subtracts an adaptive term $k_{\hat{M}_t}$, which can be viewed as an uncertainty penalty – the larger $k_{\hat{M}_t}$, the less likely the CUSUM statistic will increase. The updated CUSUM statistic is then compared against its corresponding threshold, and if it exceeds the threshold, an OOD event is declared.

VI. EXPERIMENTS

A. Experimental Setup

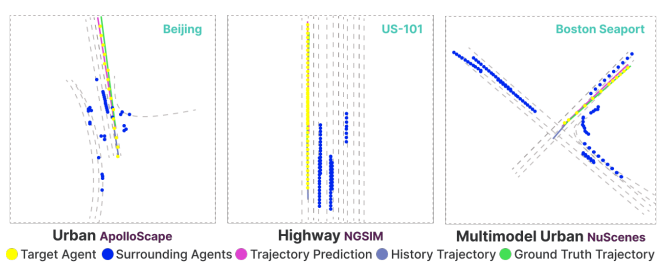


Fig. 5: Three evaluation datasets: ApolloScape (dense urban interactions), NGSIM (freeway driving), and nuScenes (multimodal urban scenes).

TABLE I: OOD detection results (mean \pm std.) on GRIP++ and FQA. Our **Mode-Aware CUSUM** achieves the best AUROC (area under ROC, higher ranking accuracy) and AUPR (area under precision-recall, robustness under class imbalance), consistently surpassing all baselines. Compared to Global CUSUM, it also produces markedly fewer false positives at high recall.

Method	GRIP++		FQA	
	AUROC	AUPR(10^{-1})	AUROC	AUPR(10^{-1})
IGMM	0.782 ± 0.006	0.314 ± 0.018	0.805 ± 0.004	0.372 ± 0.012
NLL	0.478 ± 0.003	0.075 ± 0.001	0.525 ± 0.006	0.182 ± 0.004
Global CUSUM	0.871 ± 0.009	0.528 ± 0.066	0.889 ± 0.014	0.755 ± 0.082
Mode-Aware CUSUM	0.934 ± 0.007	1.112 ± 0.139	0.948 ± 0.010	1.945 ± 0.165

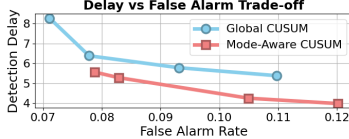


Fig. 6: Detection delay versus false alarm rate. *Mode-Aware CUSUM*(Red) shifts the trade-off curve downward relative to Global CUSUM(Blue), enabling faster detection without increasing false alarms.

Datasets and Model Selection. We evaluate our *Mode-Aware CUSUM* across datasets and models chosen for diversity in traffic, interactions, sensing, and architecture:

- **ApolloScape (Urban)** [42]. Urban traffic in Beijing, with dense mixed agent interactions (vehicles, pedestrians, riders), annotated trajectories from 1-minute camera/LiDAR sequences. High variability in interactions makes it suitable for testing rapid mode transitions.
- **NGSIM (Highway)** [43]. Freeway datasets (e.g. I-80, US-101) with long stretches of steady motion interspersed with lane changes or merges. Good for evaluating detection under mostly stable modes.
- **nuScenes (Multimodal Urban)** [44]. Urban driving in Boston and Singapore, full sensor coverage (cameras, LiDAR, radar), many object types, varied environmental conditions. Useful for handling sensor uncertainty and interaction stochasticity.

For trajectory prediction models, we select:

- **GRIP++** [40]. A graph-based, two-layer GRU model that excels on short and long horizon forecasts. We adopt a distance threshold $D_{\text{close}} = 25$ feet as in the original work to filter out distant agents.
- **FQA** [41]. Uses fuzzy attention integrating fuzzy rules with learned attention weights, allowing adaptive weighting of agent interactions. Suitable for complex urban scenes like nuScenes.

B. Results and Analysis

Q1: Does mode adaptation improve OOD detection? To ensure comparability with established OOD benchmarks, we evaluate using AUROC and AUPR [23], [8], with a *Global CUSUM* baseline that applies a single threshold across all driving scenarios [1]. Real-world datasets reveal that prediction errors vary across motion modes (detailed see Section III-A). To capture this, we propose an *Mode-Aware CUSUM* (Algorithm 1), which assigns mode-specific thresholds based

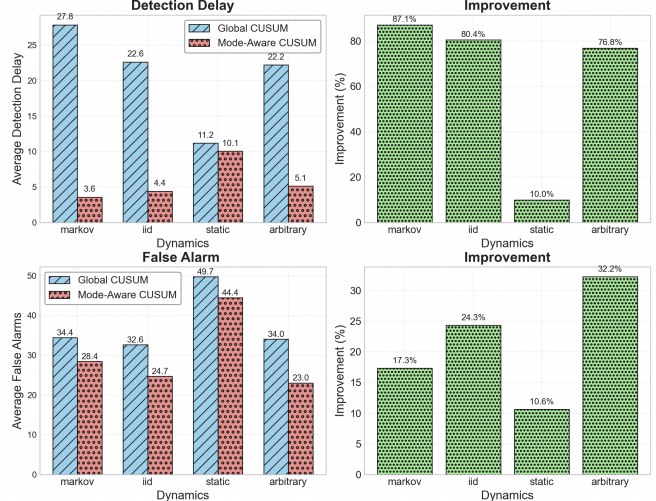


Fig. 7: Performance comparison (delay & false alarm) between Mode-Aware CUSUM (ours) and Global CUSUM. Evaluated on synthetic ApolloScape GRIP++ trajectories under four regimes: Markovian, i.i.d., static, and arbitrary.

on latent error distributions, enabling more precise OOD detection. As shown in Table I, our method consistently outperforms likelihood-based baselines (IGMM [18], NLL [24]) and Global CUSUM, achieving up to 7.2% AUROC gain and 150%+ AUPR improvement across GRIP++ and FQA. These results confirm that mode adaptation significantly boosts sequential OOD detection accuracy.

Q2: How does mode awareness affect the false alarm-delay trade-off? We evaluate *Mode-Aware CUSUM* against the *Global CUSUM* under varying false-alarm constraints, parameterizing thresholds with the exact pre-change distributions as ground truth. Experiments span all three datasets and two models, with representative results shown for GRIP++ on the ApolloScape Beijing dataset. As shown in Fig. 6, *Mode-Aware CUSUM* consistently achieves shorter detection delays at matched false alarm levels compared to *Global CUSUM*. Physically, this means that when traffic dynamics transition—for instance, from free-flowing low-risk conditions to congested high-risk states—the *Mode-Aware* detector reacts more rapidly, reducing the window of vulnerability before corrective action.

Q3: How do state dynamics affect detection robustness? As shown in Table ??, the proposed *Mode-Aware CUSUM* consistently outperforms the global baseline across all four

TABLE II: Comparison of Global CUSUM and Mode-Aware CUSUM (ours) across dynamic scenarios. Detection Delay and False Alarms are reported, with percentage improvements of Mode-Aware CUSUM over the baseline. A ↓ indicates a lower (better) value. Best values are highlighted in **bold**.

Scenario	Global CUSUM		Mode-Aware CUSUM		Improvement (%)	
	Delay↓	FAR↓	Delay↓	FAR↓	Delay	FAR
Markovian	12.5	0.18	8.2	0.12	34.4	33.3
i.i.d.	10.9	0.21	7.0	0.14	35.8	33.3
Static	15.3	0.20	9.5	0.13	37.9	35.0
Arbitrary	13.8	0.22	8.9	0.15	35.5	31.8

dynamics, yielding substantial reductions in both detection delay and false alarms. In the *Markovian* dynamic, where error modes exhibit persistent temporal structure, our method reduced detection delay by 87.1% while lowering false alarms by 17.4%, underscoring the benefit of mode-specific thresholds for capturing sustained shifts without spurious alerts. In the *IID* dynamic, characterized by highly stochastic mode switching, delay dropped by 80.4% and false alarms by 24.2%, highlighting robustness under unpredictable scene variability. Improvements in the *static* dynamic were more modest, with a 10.0% reduction in delay and 10.7% reduction in false alarms, reflecting the challenge of detecting changes in stationary environments where thresholds are rarely activated. Finally, in the *arbitrary* dynamic, the most complex regime, our detector achieved a 76.8% reduction in delay and the largest false alarm reduction of 32.4%, demonstrating strong adaptability to diverse and unpredictable patterns. Collectively, these results validate that explicitly modeling mode-specific temporal dependencies substantially enhances detection robustness across varied environments by preventing both delayed detections and spurious alarms.

C. Discussion and Takeaways

- 1) **One-Size-Fits-All OOD Detection is Suboptimal:** A general OOD detector is either too sensitive (causing false alarms in simple scenes) or not sensitive enough (missing critical events in complex scenes). Adaptation is necessary for robust performance.
- 2) **Proposed Method is Effective and Generalizable:** Our adaptive Mode-Aware framework successfully adapts to diverse driving environments. It provides faster, more accurate OOD detection without a proportional increase in false alarms, demonstrating its potential for enhancing the safety and reliability of autonomous driving systems.

VII. CONCLUSION

We addressed the challenge of OOD detection in AV’s trajectory prediction. Moving beyond prior frame-wise OOD methods and single global change detectors, we propose an *adaptive multi-threshold change-point detection algorithm (Mode-Aware CUSUM)* that explicitly models the temporal and modal dynamics of prediction errors. This is a modular architecture with mode-specific thresholds, enabling adaptation across high/low error while remaining compatible with diverse prediction models. Experiments show that our approach achieves faster and more reliable detection than global, non-adaptive methods, reducing delays and false

alarms across datasets. It also outperforms existing UQ- and vision-based baselines at higher accuracy. Overall, this work provides a practical and powerful pathway toward enhancing the safety and robustness of autonomy systems by enabling them to recognize and react to underrepresenting scenes more intelligently. Future work will explore online learning of error modes and extend the framework to a wider range of anomalous driving behaviors.

REFERENCES

- [1] T. Guo, T. Banerjee, R. Liu, and L. Su, “Building real-time awareness of out-of-distribution in trajectory prediction for autonomous vehicles,” *arXiv preprint arXiv:2409.17277*, 2024.
- [2] R. Yang, Y. Xu, Y. Fu, and L. Su, “Sstp: Efficient sample selection for trajectory prediction,” *arXiv preprint arXiv:2409.17385*, 2024.
- [3] Y. Xu, R. Yang, Y. Zhang, Y. Wang, J. Lu, M. Zhang, L. Su, and Y. Fu, “Trajectory prediction meets large language models: A survey,” *arXiv preprint arXiv:2506.03408*, 2025.
- [4] J. Nitsch, M. Itkina, R. Senanayake, J. Nieto, M. Schmidt, R. Siegwart, M. J. Kochenderfer, and C. Cadena, “Out-of-distribution detection for automotive perception,” in *2021 IEEE International Intelligent Transportation Systems Conference (ITSC)*, 2021, pp. 2938–2943.
- [5] Y. Shoeib, A. Nowzad, and H. Gottschalk, “Out-of-distribution segmentation in autonomous driving: Problems and state of the art,” in *Proceedings of the Computer Vision and Pattern Recognition Conference*, 2025, pp. 4310–4320.
- [6] Y.-C. Hsu, Y. Shen, H. Jin, and Z. Kira, “Generalized odin: Detecting out-of-distribution image without learning from out-of-distribution data,” in *Proceedings of the IEEE/CVF conference on computer vision and pattern recognition*, 2020, pp. 10951–10960.
- [7] H. Choi, E. Jang, and A. A. Alemi, “Waic, but why? generative ensembles for robust anomaly detection,” *arXiv preprint arXiv:1810.01392*, 2018.
- [8] W. Liu, X. Wang, J. Owens, and Y. Li, “Energy-based out-of-distribution detection,” *Advances in neural information processing systems*, vol. 33, pp. 21 464–21 475, 2020.
- [9] L. Kong, S. Xie, H. Hu, L. X. Ng, B. Cottreau, and W. T. Ooi, “Robodepth: Robust out-of-distribution depth estimation under corruptions,” *Advances in Neural Information Processing Systems*, vol. 36, pp. 21 298–21 342, 2023.
- [10] A. Zyner, S. Worrall, and E. Nebot, “A recurrent neural network solution for predicting driver intention at unsignalized intersections,” *IEEE Robotics and Automation Letters*, vol. 3, no. 3, pp. 1759–1764, 2018.
- [11] W. Ding, J. Chen, and S. Shen, “Predicting vehicle behaviors over an extended horizon using behavior interaction network,” in *2019 international conference on robotics and automation (ICRA)*. IEEE, 2019, pp. 8634–8640.
- [12] X. Li, X. Ying, and M. C. Chuah, “Grip: Graph-based interaction-aware trajectory prediction,” in *2019 IEEE Intelligent Transportation Systems Conference (ITSC)*. IEEE, 2019, pp. 3960–3966.
- [13] Z. Zhao, H. Fang, Z. Jin, and Q. Qiu, “Gisnet: Graph-based information sharing network for vehicle trajectory prediction,” in *2020 International Joint Conference on Neural Networks (IJCNN)*. IEEE, 2020, pp. 1–7.
- [14] A. Postnikov, A. Gamayunov, and G. Ferrer, “Transformer based trajectory prediction,” *arXiv preprint arXiv:2112.04350*, 2021.
- [15] F. Amin, K. Gharami, and B. Sen, “Trajectoformer: Transformer-based trajectory prediction of autonomous vehicles with spatio-temporal neighborhood considerations,” *International Journal of Computational Intelligence Systems*, vol. 17, no. 1, p. 87, 2024.

- [16] J. Liang, C. Tan, L. Yan, J. Zhou, G. Yin, and K. Yang, "Interaction-aware trajectory prediction for safe motion planning in autonomous driving: A transformer-transfer learning approach," *IEEE Transactions on Intelligent Transportation Systems*, 2025.
- [17] Z. Wang, G. Zhang, T. Sun, C. Shi, and B. Zhou, "Data-driven methods for low-dimensional representation and state identification for the spatiotemporal structure of cavitation flow fields," *Physics of fluids*, vol. 35, no. 3, 2023.
- [18] J. Wiederer, J. Schmidt, U. Kressel, K. Dietmayer, and V. Belagiannis, "Joint out-of-distribution detection and uncertainty estimation for trajectory prediction," in *2023 IEEE/RSJ International Conference on Intelligent Robots and Systems (IROS)*. IEEE, 2023, pp. 5487–5494.
- [19] A. Nayak, A. Eskandarian, Z. Doerzaph, and P. Ghorai, "Pedestrian trajectory forecasting using deep ensembles under sensing uncertainty," *IEEE Transactions on Intelligent Transportation Systems*, vol. 25, no. 9, pp. 11 317–11 329, 2024.
- [20] Y. Cao, D. Xu, X. Weng, Z. Mao, A. Anandkumar, C. Xiao, and M. Pavone, "Robust trajectory prediction against adversarial attacks," in *Conference on robot learning*. PMLR, 2023, pp. 128–137.
- [21] Q. Zhang, S. Hu, J. Sun, Q. A. Chen, and Z. M. Mao, "On adversarial robustness of trajectory prediction for autonomous vehicles," in *Proceedings of the IEEE/CVF Conference on Computer Vision and Pattern Recognition*, 2022, pp. 15 159–15 168.
- [22] J. Wiederer, J. Schmidt, U. Kressel, K. Dietmayer, and V. Belagiannis, "Joint out-of-distribution detection and uncertainty estimation for trajectory prediction," in *2023 IEEE/RSJ International Conference on Intelligent Robots and Systems (IROS)*, 2023, pp. 5487–5494.
- [23] D. Hendrycks and K. Gimpel, "A baseline for detecting misclassified and out-of-distribution examples in neural networks," *arXiv preprint arXiv:1610.02136*, 2016.
- [24] K. Lee, K. Lee, H. Lee, and J. Shin, "A simple unified framework for detecting out-of-distribution samples and adversarial attacks," *Advances in neural information processing systems*, vol. 31, 2018.
- [25] Y. Sun, Y. Ming, X. Zhu, and Y. Li, "Out-of-distribution detection with deep nearest neighbors," in *International Conference on Machine Learning*. PMLR, 2022, pp. 20 827–20 840.
- [26] P. Cui and J. Wang, "Out-of-distribution (ood) detection based on deep learning: A review," *Electronics*, vol. 11, no. 21, p. 3500, 2022.
- [27] B. Lakshminarayanan, A. Pritzel, and C. Blundell, "Simple and scalable predictive uncertainty estimation using deep ensembles," *Advances in neural information processing systems*, vol. 30, 2017.
- [28] Y. Gal and Z. Ghahramani, "Dropout as a bayesian approximation: Representing model uncertainty in deep learning," in *international conference on machine learning*. PMLR, 2016, pp. 1050–1059.
- [29] A. Nayak, A. Eskandarian, and Z. Doerzaph, "Uncertainty estimation of pedestrian future trajectory using bayesian approximation," *IEEE Open Journal of Intelligent Transportation Systems*, vol. 3, pp. 617–630, 2022.
- [30] V. V. Veeravalli and T. Banerjee, "Quickest change detection," in *Academic press library in signal processing*. Elsevier, 2014, vol. 3, pp. 209–255.
- [31] P. Yang, G. Dumont, and J. M. Ansermino, "Adaptive change detection in heart rate trend monitoring in anesthetized children," *IEEE transactions on biomedical engineering*, vol. 53, no. 11, pp. 2211–2219, 2006.
- [32] R. Malladi, G. P. Kalamangalam, and B. Aazhang, "Online bayesian change point detection algorithms for segmentation of epileptic activity," in *2013 Asilomar conference on signals, systems and computers*. IEEE, 2013, pp. 1833–1837.
- [33] A. G. Tartakovsky, A. S. Polunchenko, and G. Sokolov, "Efficient computer network anomaly detection by changepoint detection methods," *IEEE Journal of Selected Topics in Signal Processing*, vol. 7, no. 1, pp. 4–11, 2012.
- [34] A. Tartakovsky, I. Nikiforov, and M. Basseville, *Sequential analysis: Hypothesis testing and changepoint detection*. nill: CRC press, 2014.
- [35] T. Banerjee and V. V. Veeravalli, "Data-efficient quickest change detection in minimax settings," *IEEE Transactions on Information Theory*, vol. 59, no. 10, pp. 6917–6931, 2013.
- [36] G. V. Moustakides, "Optimal stopping times for detecting changes in distributions," *the Annals of Statistics*, vol. 14, no. 4, pp. 1379–1387, 1986.
- [37] G. Lorden, "Procedures for reacting to a change in distribution," *The annals of mathematical statistics*, pp. 1897–1908, 1971.
- [38] M. F. R. Chowdhury, S.-A. Selouani, and D. O'Shaughnessy, "Bayesian on-line spectral change point detection: a soft computing approach for on-line asr," *International Journal of Speech Technology*, vol. 15, pp. 5–23, 2012.
- [39] A. G. Tartakovsky, B. L. Rozovskii, R. B. Blažek, and H. Kim, "Detection of intrusions in information systems by sequential change-point methods," *Statistical methodology*, vol. 3, no. 3, pp. 252–293, 2006.
- [40] X. Li, X. Ying, and M. C. Chuah, "Grip++: Enhanced graph-based interaction-aware trajectory prediction for autonomous driving," *arXiv preprint arXiv:1907.07792*, 2019.
- [41] N. Kamra, H. Zhu, D. K. Trivedi, M. Zhang, and Y. Liu, "Multi-agent trajectory prediction with fuzzy query attention," *Advances in Neural Information Processing Systems*, vol. 33, pp. 22 530–22 541, 2020.
- [42] X. Huang, X. Cheng, Q. Geng, B. Cao, D. Zhou, P. Wang, Y. Lin, and R. Yang, "The apolloscape dataset for autonomous driving," in *Proceedings of the IEEE conference on computer vision and pattern recognition workshops*. nill: nill, 2018, pp. 954–960.
- [43] Federal Highway Administration. (2020) Traffic analysis tools: Next generation simulation. nill. [Accessed: Sep. 13, 2024]. [Online]. Available: <https://ops.fhwa.dot.gov/trafficanalysis/tools/ngsim.htm>
- [44] H. Caeser, V. Bankiti, A. H. Lang, S. Vora, V. E. Liong, Q. Xu, A. Krishnan, Y. Pan, G. Baldan, and O. Beijbom, "nuscenes: A multimodal dataset for autonomous driving," in *Proceedings of the IEEE/CVF conference on computer vision and pattern recognition*. nill: nill, 2020, pp. 11 621–11 631.
- [45] H. Kim, D. Kim, G. Kim, J. Cho, and K. Huh, "Multi-head attention based probabilistic vehicle trajectory prediction," in *2020 IEEE Intelligent Vehicles Symposium (IV)*. IEEE. nill, 2020, pp. 1720–1725.
- [46] N. Deo and M. M. Trivedi, "Convolutional social pooling for vehicle trajectory prediction," in *Proceedings of the IEEE conference on computer vision and pattern recognition workshops*. nill: nill, 2018, pp. 1468–1476.
- [47] J. Bao, Y. Li, M. Zhu, and S. Wang, "Bayesian nonparametric hidden markov model for agile radar pulse sequences streaming analysis," *IEEE Transactions on Signal Processing*, vol. 71, pp. 3968–3982, 2023.
- [48] T. M. Cover, *Elements of information theory*. John Wiley & Sons, 1999.